Article

Identification of Biologically Active Pyrimido[5,4-*b*] indoles that Prolong NF-#B Activation Without Intrinsic Activity

Michael Chan, Alast Ahmadi, Shiyin Yao, Fumi Sato-Kaneko, Karen Messer, Minya Pu, Brandon Nguyen, Tomoko Hayashi, Maripat Corr, Dennis Carson, Howard B. Cottam, and Nikunj Shukla

ACS Comb. Sci., **Just Accepted Manuscript** • DOI: 10.1021/acscombsci.7b00080 • Publication Date (Web): 28 Jun 2017

TOC GRAPHIC

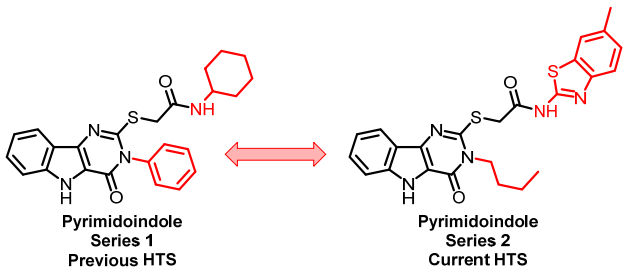

Bio-activity	Series 1	Series 2
Toll-like Receptor 4 Agonist	Yes	No
Intrinsic NF-κB Activity	Yes	No
Sustain NF-κB Activation by LPS	No	Yes

Identification of Biologically Active Pyrimido[5,4-*b*] indoles that Prolong NF-κB Activation Without Intrinsic Activity

Michael Chan,[a] *Alast Ahmadi,*[a] *Shiyin Yao,*[a] *Fumi Sato-Kaneko,*[a] *Karen Messer,*[b] *Minya Pu,*[b] *Brandon Nguyen,*[a] *Tomoko Hayashi,*[a] *Maripat Corr,*[c] *Dennis A. Carson,*[a] *Howard B. Cottam,*[a] *Nikunj M. Shukla*,*[a]

a. Moores UCSD Cancer Center, University of California San Diego, La Jolla, CA 92093, USA.

b. Division of Biostatistics, University of California San Diego, La Jolla, CA 92093, USA.

c. Department of Medicine, University of California San Diego, La Jolla, CA 92093, USA.

KEYWORDS: adjuvant, pyrimidoindole, NF-κB, LPS, TLR4

ABSTRACT

Most vaccine adjuvants directly stimulate and activate antigen presenting cells, but do not sustain immunostimulation of these cells. A high throughput screening (HTS) strategy was designed to identify compounds that would sustain NF-κB activation by a stimulus from toll-like receptor (TLR)4 ligand, lipopolysaccharide (LPS). Several pilot studies optimized the parameters and conditions for a cell based NF-κB reporter assay in human monocytic THP-1 cells. The final assay evaluated prolongation of LPS induced NF-κB activation at 12h (hours). The dynamic range of the assay was confirmed in a pilot screen of 14,631 compounds, and subsequently in a main extensive screen with 166,304 compounds. Hit compounds were identified using an enrichment strategy based on unsupervised chemoinformatic clustering, and also by a naïve 'Top X' approach. 2,011 compounds were then rescreened for levels of co-activation with LPS at 5h and 12h, which provided kinetic profiles. Of the 407 confirmed hits, compounds that showed correlation of the kinetic profiles with the structural similarities led to identification of four chemotypes: pyrimido[5,4-*b*]indoles; 4*H*-chromene-3-carbonitriles; benzo[*d*][1,3]dioxol-2-ylureas; and tetrahydrothieno[2,3-*c*]pyridines, which were segregated by 5h and 12h kinetic characteristics. Unlike the TLR4 agonistic pyrimidoindoles identified in previous studies, the revealed pyrimidoindoles in the present work did not intrinsically stimulate TLR4 nor induce NF-κB, but rather prolonged NF-κB signaling induced by LPS. A 42-member combinatorial library was synthesized which led to identification of potent *N*3-alkyl substituted pyrimidoindoles that were not only active *in vitro* but also enhanced antibody responses *in vivo* when used as a co-adjuvant. The novel HTS strategy led to identification of compounds that are intrinsically quiescent but functionally prolong stimulation by a TLR4 ligand and thereby potentiate vaccine efficacy.

Introduction: The dearth of adjuvants in human vaccines has motivated the search for effective non-toxic immunomodulators that provide sustained immunoprotection particularly to high-risk populations such as the elderly.[1-5] The use of Toll-like receptor (TLR) ligands has gained interest as sensors of innate immunity and stimulators of antigen-presenting cells (APCs) that prime protective immune responses.[6] The use of TLR ligands as adjuvants can provide a potent activation stimulus to resident APCs, and promote further APC recruitment to the site of antigen injection and subsequent delivery to the draining lymph nodes.[2-3] In a prior high throughput screen (HTS) using the Förster resonance energy transfer (FRET) based CellSensor® NF-κB-bla reporter in the human monocytic leukemic cell line, THP-1, we identified pyrimido[5,4-*b*]indole and 2-aminoquinazoline chemotypes that were characterized as TLR4/MD-2 ligands.[7-8] These compounds were directly immunostimulatory and provided the basis for developing a lead compound shown to be an effective adjuvant in a murine model of influenza.[9]

Other toll-like receptor ligands have also been developed as vaccine adjuvants as they are innate immune stimulators and can directly activate APCs.[2, 10-17] To initiate immune responses from vaccines, antigen-loaded activated APCs travel from the site of injection to regional lymph nodes and prime naïve T cells. During the time period that the APC travels from the vaccine injection site to a regional lymph node, the activation status is down-regulated (**Fig. 1A**, red dashed line). Activation of innate immune responses is regulated through multiple negative feedback loops.[18-20] Negative regulators of TLR signaling that have been reported to date include processing pathways (ubiquitination[21-23], degradation[24], stabilization[25]), molecular competition[20], promoter regulation[23], phosphatases[26-27], and epigenetic regulators.[28-32] For example, interleukin-1 receptor-associated kinase (IRAK)-M[20], phosphatidylinositide (PI)3 kinase inhibitors[33] and anti-inflammatory cytokines (IL-10[30] and transforming growth factor β[34]) have evolved to co-

modulate innate immune responses and inflammation.[35] These negative feedback systems may adversely impact the ability of adjuvants to sustain APC activation, and to induce optimal T lymphocyte memory responses.

Most vaccine development approaches have been to directly activate and stimulate APCs. However, prolonging the activation status of a cell by intercepting a negative regulatory pathway would be as valuable an approach to allow the impetus of the primary stimulus to be sustained during the transit time to the lymph node and to increase the number of T and B cell interactions the activated cell may have in the lymphoid environment. A compound disrupting one or more of the regulatory systems could sustain the activation status of a TLR stimulated APC. To date, HTS campaigns related to NF-κB have focused on identifying pathway inhibitors[36-41] or intrinsic activators.[7-8] However, no HTS campaign has focused on identifying compounds that sustain initial NF-κB stimulation by a TLR agonist. We hypothesized that identification of such small molecules could complement current TLR agonists as adjuvants and improve the efficacy of vaccines that are locally administered.

Results and Discussion: Overall HTS strategy and design. Here, we aimed to identify compounds that manipulate negative feedback systems to sustain innate immune activation through a classic TLR4 ligand, lipopolysaccharide (LPS). We again used the CellSensor® NF-κB-bla reporter in a human monocytic cell line, THP-1, as a model of functional monocyte-derived APCs for HTS. This cell-based assay was chosen as many of the cellular functions of APCs are retained and the dual fluorescence normalizes relative cell number and viability to NF-κB activity in each well. Typically, LPS stimulates NF-κB activation within the APC and then an increase in regulatory "deactivation" molecules (**Fig. 1A**, blue dashed line) results in a decline in activation status. We sought to find small molecules that would prolong the LPS induced

activation status by reducing or inhibiting these negative molecular regulators (**Fig. 1A**, red and blue lines, respectively).

To identify compounds that prolonged the activation of APCs by LPS, we developed a tiered HTS strategy (**Fig. 1B**). First, the conditions for the THP-1 CellSensor® NF-κB-bla assay were optimized for a 12h stimulation assay with LPS as described below. An initial pilot screen was performed with 14,631 representative compounds to evaluate the performance of the assay and quality control. The main HTS was then performed with a collection of 166,304 compounds that included the compounds used in the pilot screen to verify the reproducibility of the assay. We utilized our previously reported structure-based cluster analysis to select 2,011 compounds for confirmation.[42] These compounds were tested in duplicate in a confirmation screen for prolonged activation at 12h, but we also included an additional 5h screen to evaluate the kinetics of the stimulatory response. Approximately 20% (407 compounds) were confirmed as hits and substructure based clustering broadly classified some of these compounds into four chemotypes: pyrimido[5,4-*b*]indoles; 4*H*-chromene-3-carbonitriles; benzo[*d*][1,3]dioxol-2-ylureas; and tetrahydrothieno[2,3-c]pyridines. As we had prior success with developing a pyrimidoindole as a lead compound, this class was selected for further structure-activity relationship (SAR) studies.

Assay optimization: For our LPS co-stimulation strategy we optimized the THP-1 CellSensor® NF-κB-bla assay for variables including: 1) cell number; 2) preincubation time of thawed cells; 3) concentration of FBS; 4) incubation time; and 5) the dose and timing of a positive control compound, wortmannin, a PI3 kinase inhibitor that has been reported to augment initial NF-κB activity.[43-45] In the first set of experiments, the tissue culture fetal bovine serum (FBS) concentration was kept constant at 10% while cell numbers were varied between 10,000 cells/well and 20,000 cells/well, and the preincubation time of thawed cells was either -16h or 0h

relative to test compound and LPS addition (**Fig. 2A**). In addition, FRET response ratios were measured after 24h for 100ng/mL LPS co-incubated with graded concentrations of wortmannin in the above-mentioned four different cell plating conditions. Higher FRET ratios were reliably demonstrated with 20,000 cells/well and a 16h preincubation time of the thawed cells (**Fig. 2A**). The potential for individual test compounds to bind to bovine albumin and other proteins in FBS could lead to a false negative output, so we probed the effect of lowering the FBS concentration (5%, 2% or 1%) on prolonged LPS stimulation in the presence of graded concentrations of wortmannin (**Fig. 2B**). Response ratios decreased with reduced concentrations of FBS and also at higher concentrations of wortmannin (**Fig. 2B**). Thus, 5% FBS concentration was determined to be optimum for the assay.

As the optimal incubation period of THP-1 Cellsensor® NF-κB recommended by the manufacturer is 5h to 6h, a longer incubation time with THP-1 cells may lead to cellular stress responses as well as degradation of compounds due to metabolism. We were therefore interested to find the optimum incubation time to allow for natural decay of the LPS stimulation without losing the ability to distinguish an increase in the FRET signal due to aberrations in cellular metabolism or cell death. Using the previously optimized parameters (20,000 cells/well and 5% FBS), response ratios were measured at 6, 12, 18 and 24h after stimulation with100ng/mL LPS alone (**Fig. 2C**). In addition, LPS was added after 18h (LPS last) in untreated cells and the response ratio was measured after 6h to verify retention of the FRET activity in the cells after a long incubation time. LPS stimulation results in activation at 6h; however, the response ratio shows a significant drop at 12h which reached a plateau at later time points. The response ratio for LPS at 6h and for 'LPS last' are almost identical suggesting that THP-1 cells do not lose

activity even after longer incubation time (**Fig. 2C**). As there was no difference at 12h and later time points we chose 12h for the HTS.

Next, we varied the dose and time of wortmannin (as a test compound) addition relative to LPS. Wortmannin at graded doses was added either 1h before, or at 0, 2 and 4h after the addition of LPS. The response ratios were higher when wortmannin was added before or with LPS, but the signal decreased when wortmannin was added 2h or 4h after LPS (**Fig. 2D**). Thus, the addition of 0.25μM wortmannin concurrent with 100ng/mL LPS was chosen as optimal for the assay. The final optimized conditions for the HTS to identify compounds that prolong initial activation of NF-κB by LPS are summarized in a schematic protocol (**Fig. 2E**).

Pilot screen and HTS: Using the optimized assay conditions, a pilot screen was first performed using 14,631 compounds selected to represent the diversity of the libraries in the chemical collection at University of California San Francisco (UCSF) Small Molecule Discovery Center (SMDC). The screen was performed using LPS alone (LPS 12h) and LPS + 0.25 μM wortmannin as a positive control, 0.5% DMSO (no LPS) as a negative control and an additional control included adding LPS at 5h before adding substrate (LPS 5h). The percent activation calculated using LPS 5h as reference is shown in **Fig. 3A**. Statistical analysis showed good quality for the different controls and we proceeded with the main screen, which included 166,304 test compounds on 527 plates. In addition, 27 plates containing 8,627 compounds from the pilot screen were re-screened in triplicate within the main screen, in order to provide quality control information and to estimate confirmation rates. The percent activation plot for the main screen (**Fig. 3B**) showed inter-plate variability for the LPS control (LPS 12h). To mitigate for the variability, we calculated values based on the LPS control within each plate. Intra-plate calculations for 'distance to LPS' was calculated and used as the metric for compound selection.

The main screen median Z' was 0.74 (0.43 to 0.90). As in prior work, we used cluster enrichment methods including Murcko scaffold classes, Daylight functional clusters, and Top X approach, to identify 2,011 compounds for the confirmation and kinetic profiling screens (**Supporting Information, Fig. S1**).[42]

Confirmation screen and kinetic profiling: The selected hits from the main screen were then evaluated in duplicate in a confirmation screen at 12h and an additional screen at 5h for kinetic profiling. **Fig. 4A** shows a scatter plot of the data (distance to LPS) for these compounds from the 12h confirmation screen on the ordinate axis and from 5h kinetic profiling screen on the abscissa axis. 407 compounds were identified as confirmed hits from the 12h screen using a data-driven method that fits a mixture of two linear models utilizing both the primary and confirmation screen data for these compounds. All of the confirmed hits enhanced NF-κB induction activity of LPS at 12h and were broadly classified into four groups showing 4 general kinetic patterns (**Fig. 4B**). Based on 5h screen, these compounds were either early inhibitors (5h distance to LPS<0) or early enhancers (5h distance to LPS>0). Within the early inhibitors, the compounds were grouped as either showing moderate increase or high increase in NF-κB induction compared to LPS at 12h (green and orange symbols, respectively, **Fig. 4A**), where cut-off used was mean+SD of the LPS 5h values from all the confirmation screen plates. Similarly, within the enhancer groups, compounds showed either moderate or high increases in NF-κB induction compared to LPS at 12h (red and blue symbols, respectively, **Fig. 4A**). Theoretical activation profiles for these groups of compounds are shown in **Fig. 4B** with the same color patterns**.** The structures of these compounds were then subjected to substructure based clustering using the server based ChemMine tools (University of California, Irvine; http://chemmine.ucr.edu/tools/launch_job/Clustering/) and binning clustering application with a

similarity cutoff of 0.5. The application allowed us to group these compounds into several chemotypes and correlation of kinetic profiles with structural similarities led us to identify four major structural classes, namely: pyrimido[5,4-*b*]indoles; 4*H*-chromene-3-carbonitriles; benzo[*d*][1,3]dioxol-2-ylureas; and tetrahydrothieno[2,3-*c*]pyridines (**Fig. 4C**). Most of the compounds in pyrimido[5,4-*b*]indole and tetrahydrothieno[2,3-*c*]pyridine series were early enhancers while the bulk of the compounds in the 4*H*-chromene-3-carbonitriles and benzo[*d*][1,3]dioxol-2-ylureas series were early inhibitors, as described earlier. **Fig. 4C** shows the distribution of the compounds in a chemotype connected to a calculated geometric centroid from the coordinates of the individual compounds. The centroid for these four different chemotypes clearly lies in the four different regions with distinct kinetic activation profiles as shown in **Fig. 4B**.

Structure-activity relationship studies on pyrimidoindoles: Pyrimidoindoles were identified as TLR4/MD2 agonists in a previous HTS,[7, 42] which was designed to identify compounds that induced NF-κB activation. The identification of this chemotype here as prolonging NF-κB induction warranted additional investigation into the structural differences to understand functional characteristics. Overall, 536 pyrimidoindoles were evaluated in both the HTS campaigns, the bulk of which consisted of 357 amide-linked compounds (66.6%) and a small fraction of 27 ester-linked compounds (5%). Within the amide-linked compounds, there was a relatively higher number of *N*3-aryl (297 compounds) versus *N*3-methyl (60 compounds) substituted pyrimidoindoles pointing toward a bias for *N*3-aryl derivatives. A plot of potency signatures for the current HTS (distance to LPS) on the y-axis against previous HTS[42] (percent activation) on the x-axis showed a clear demarcation for pyrimidoindoles designated as 'hits' in the two different but related assays (**Fig. 5**). The amide-linked hits identified in the previous HTS

showed high dominance for *N*3-aryl substitution (73%) nearly matching the ratio present in the HTS library, however the amide-linked hits identified in the current HTS had a very high dominance for *N*3-methyl substitution (62%), despite being low in number (**Fig. 5**). In addition, the current HTS also identified two active ester-linked compounds. Here, it is important to distinguish between the two HTS campaigns relative to the pyrimidoindoles chemotype. The first campaign was designed to identify compounds that alone had intrinsic ability to activate NF-κB, and as mentioned above, pyrimidoindoles bearing *N*3-aryl substitutions were found in this category, whereas those compounds bearing the *N*3-methyl substituent were inactive in the prior screen. In contrast, the present campaign was designed to identify compounds that could enhance or prolong an already-present TLR4 innate immune stimulus (LPS), and in this category, several pyrimidoindoles bearing *N*3-methyl substituent were found to be active. With this in mind, we decided to pursue a combinatorial library of 42 compounds to explore a homologous series of *N*3-alkyl substitutions including *N*3-methyl, -ethyl, -propyl, -butyl, -isopropyl, and *N*3-aryl substitutions including *N*3-*p*-fluorophenyl and -*p*-methoxyphenyl. The other variation in the combinatorial library consisted of three esters (methyl, ethyl and *tert*-butyl) and three amides linked to 2-amino substituent of thiazole, benzothiazole and 6-methylbenzothiazole at the C2 position as these substituents were identified as most potent in both the main and the 12h confirmation screens.

The proposed compounds were synthesized as shown in **Scheme 1**. The common precursor ethyl 3-amino-1*H*-indole-2-carboxylate (**1**) was reacted with isothiocyanate chemset **2**{1-7} to obtain the intermediate thiourea chemset **3**{1-7}, followed by intramolecular condensation to yield the fused pyrimidine ring using acetyl chloride and ethanol to obtain chemset **4**{1-7}. These compounds were then reacted with three different 2-chloroacetates **5**{1-3} and 2-

chloroacetamides **5**{4-6} to obtain the 42 compound combinatorial library of differently *N*3 and C2 substituted pyrimidoindoles **6**{1-7, 1-6}.

These compounds were tested in the Cellsensor® THP-1 cells at 5μM concentration for enhancement of NF-κB upregulation with LPS at 5h and 12h. The activity data was calculated as percent activation (%act), which was measured as FRET response ratios relative to the LPS alone control (**Supporting Information**, **Table S1**). None of the synthesized compounds significantly enhanced NF-κB induction at 5h, while all the ester linked derivatives and thiazole amide linked compounds **6**{1-7, 1-4} showed negligible increases in NF-κB induction at 12h compared to LPS alone. However, some of the amide-linked compounds with the 2-aminobenzothiazole and 2-amino-6-methylbenzothiazole substituents (**6**{1-7, 5-6}) were very active and showed a distinct relationship between the *N*3-alkyl chain length and the NF-κB inducing activities in presence of LPS at 12h. In *N*3-alkyl substituted benzothiazole derivatives **6**{3-7, 5} the percent activation value increases moderately for *N*3-methyl (**6**{4,5}, %act=100), *N*3-ethyl (**6**{5,5}, %act=120), *N*3-propyl (**6**{6,5}, %act=119) derivatives; however, the *N*3-butyl derivative (**6**{4,5}, %act=180) was found to be the most potent, and surprisingly the *N*3-isopropyl derivative (**6**{3,5}, %act=75) showed NF-κB inhibitory effects with values lower than that of LPS alone. A similar trend was observed with the *N*3-alkyl substituted methylbenzothiazole derivatives **6**{3-7, 6} with both the *N*3-propyl and *N*3-butyl substituted derivatives being very potent (**6**{6,6}, %act=190, **6**{7,6}, %act=192 respectively). The *N*3-isopropyl derivative (**6**{3,6}, %act=85) with LPS showed reduction in NF-κB activation compared to the LPS alone suggesting that branched alkyl chain is not tolerated. In the *N*3-aryl substituted derivatives, the 4-flouorphenyl substituted compounds (**6**{1,5-6}) exhibited better potency than the corresponding 3-methoxyphenyl substituted analogs (**6**{2,5-6}).

Next, we assayed the toxicity of these compounds in THP-1 cells using an (3-(4,5-dimethylthiazol-2-yl)-2,5-diphenyltetrazolium bromide) MTT assay. Toxicity was measured as percent viability relative to the vehicle, (0.5% DMSO). All of the weakly potent ester-linked compounds were found to be non-toxic (%viability>90) at 5μM, while all of the thiazole substituted amide-linked compounds were found to be relatively toxic suggesting an off-target effect related to the presence of the thiazole group. Among the *N*3-alkyl substituted benzothiazole or 6-methylbenzothiazole derivatives, all except the *N*3-propyl and -isopropyl derivatives were relatively more toxic.

In order to identify an optimum *N*3-alkyl chain length for maximal potency, we synthesized *N*3-pentyl (**9a** and **10a**) and hexyl (**9b** and **10b**) derivatives for the benzothiazole and 6-methylbenzothiazole substituted compounds as shown in **Scheme 2**. These higher chain analogs showed declining potency with increasing chain length (**9a**; %act=154, **9b;**%act=143, **10a**; %act=139, **10b**; %act=142) and also were found to be relatively more toxic. We had earlier reported that *N*5-methylation of pyrimidoindoles reduces their toxicity without abrogating the activity at TLR4.[7] Thus, we synthesized *N*5-methyl derivatives of the potent *N*3-butyl substituted derivatives **6**{7, 5-6}. These compounds, however, did not eliminate toxicity, but lost their ability to sustain an LPS induced NF-κB response (**11**; %act=94, **12**; %act=91).

Moreover, while these active *N*3-alkyl derivatives enhance the LPS induced NF-κB activation, they appear to do so by a mechanism that is independent of TLR4 binding, unlike the derivatives identified in the previous HTS. We evaluated the abilities these compounds have to activate the NF-κB and TLR4 signaling pathways using THP-1 NF-κB Cellsensor® and human TLR4 HEK reporter cell lines, respectively. We found that these compounds lack activity in either of these

assays as compared to the potent pyrimidoindoles identified in the previous HTS (**Supporting Information, Fig. S2**).

For all the above reasons, we were interested to pursue vaccination studies in mice with these novel compounds in the presence of a TLR4 stimulus to evaluate their potential co-adjuvant effects. We chose MPLA (monophosphoryl lipid A), a known TLR4 agonist and Food and Drug Administration (FDA) approved adjuvant, and ovalbumin (OVA) as antigen for the vaccination studies. Examination of antigen-specific antibodies showed that co-immunization of MPLA with compounds **6**{7,5}, **6**{6,6} or **6**{7,6} induced statistically significant increases in antigen specific IgG titers when compared to mice immunized with MPLA alone ($p<0.05$ compared to MPLA plus antigen, **Fig. 7**).

Conclusions: In conclusion, a novel HTS assay using THP-1 Cellsensor® reporter cells has been standardized and used to identify compounds that prolong NF-κB activation when co-administered with a TLR4 stimulus (LPS). Hit compounds were identified using an enrichment strategy based on unsupervised chemoinformatic clustering of the compounds within the screen library, and also by a naïve 'Top X' approach. Confirmation screening at 12h and kinetic profile screening at 5h yielded 407 confirmed hits. The correlation of the kinetic profiles with the structural similarities led to identification of four chemotypes including pyrimido[5,4-*b*]indoles. A 42-member combinatorial library of pyrimidoindoles was synthesized that led to identification of potent *N*3-alkyl substituted pyrimidoindole analogs. Although these potent compounds were intrinsically inactive towards NF-κB induction or TLR4 activation, when co-adjuvanted with MPLA, they augmented the level of antigen-specific IgG production in mice Many of the negative regulatory pathways involve kinase; hence future studies to elucidate the mechanisms of action of these derivatives will include kinase inhibitory assays among other pathways.

Experimental Methods:

Compound Library. A library of compounds was acquired from the UCSF Small Molecule Discovery Center consisting of 166,304 chemical entities from eight suppliers (**Supporting Information, Fig. S3**).

High throughput screening and Statistical Analysis. HTS was performed by Life Technologies Corporation at their commercial facility (Madison, WI) in 384 well plates using Cellsensor® THP-1 cells. The screen was performed using LPS alone (LPS 12h) and LPS + 0.25μM wortmannin as positive controls, 0.5% DMSO as negative control and an additional control included adding LPS at 5h before adding substrate (LPS 5h). There were 527 plates in the main screen, and 18 plates each in the12h confirmation screen and in the 5h kinetic screen. Emission ratios were computed as the ratio of fluorescence density values at two wavelengths, fluorescein versus coumarin emission, after background subtraction using the mean of the cell-free wells. Response ratios (RR) were computed as the emission ratio divided by the mean emission ratio from no-lipid wells within the same plate. To optimize assay parameters, box plots and bar graphs were used to describe data. For compound selection, percent activation by plate was computed as the difference between RR from a particular well and the mean RR from no-LPS (0.5% DMSO) wells, divided by the difference of the mean RRs between LPS 5h wells and no LPS (0.5% DMSO) wells. Quality checks in the pilot screen included making dot plots of percent activation values versus well number by well type, calculating Z' for each plate, making scatter plots for duplicated compounds and outlier detection. In both the main screen and the confirmation screen, to account for the variability from the LPS 12h wells (where LPS was added at 0h), distance to LPS (standardized percent activation values against LPS 12h, calculated as the difference between percent activation values for the test compound and mean of LPS 12h

control wells divided by the standard deviation for the LPS 12h control wells within each plate) was used as the metric for compound selection. In main screen, a cluster enrichment method[42] was used to identify hits where Murcko scaffold classes, Daylight functional clusters, and Top X approach (whether the distance to LPS first >3) were used together to select compounds to carry forward. In the confirmation screen, compounds were identified as confirmed hits based on a mixture of two linear models using data from both confirmation and primary screens. R (www.r-project.org, version 3.3.1) and Prism 6 (GraphPad Software, San Diego, CA) statistical software were used to carry out these analyses.[46]

Chemistry. Reagents and solvents used were obtained as at least reagent grade from commercial sources and used without further purification unless noted otherwise. Moisture or air-sensitive reactions were conducted under argon atmosphere in oven-dried (120^{o}C) glass apparatus. The solvents were removed under reduced pressure using standard rotary evaporators. Flash chromatography was carried out on a Biotage Isolera One (Charlotte, NC); while analytical thin-layer chromatography (TLC) was performed using precoated TLC silica gel 60 F254 aluminum sheets purchased from EMD (Gibbstown, NJ) and visualized using UV light. Reaction monitoring, compound characterization, and purity analysis were performed using a 1260 Infinity/6420 Triple Quad (Agilent Technologies, Inc., Santa Clara, CA) with a Supelco Discovery HS C18 column (Sigma-Aldrich). All the compounds were identified to be at least 98% pure by UV. Compounds of interest were analyzed by high resolution MS (HRMS) using an Agilent 6230 ESI-TOFMS (Santa Clara, CA). ^{1}H NMR spectra were obtained on a Varian Mercury 400 (Varian, Inc., Palo Alto, CA). ^{13}C HNMR spectra were obtained on a Varian VX 500 equipped with a Varian XSens 2 channel NMR Cold Probe (Varian, Inc., Palo Alto, CA).

The chemical shifts are expressed in parts per million (ppm) using suitable deuterated NMR solvents.

General procedure for the synthesis of Compound 3{1-7}. To a solution of compound **1** (1 eq.) in warm ethanol was added the appropriate isothiocyanate **2**{1-7} (1.1 eq.) dropwise with stirring. The reaction mixture was refluxed for 6h and then allowed to cool at 4 ^{o}C overnight. Precipitated solids were filtered, washed with ethanol and dried overnight under vacuum to yield compounds **3**{1-7} as white solids.

General procedure for the synthesis of Compound 4{1-7}. A solution of sodium ethoxide (10 eq.) was prepared in anhydrous ethanol and stirred for 5 minutes. Separately, compound **3**{1-7} was dissolved in anhydrous ethanol and added to the sodium ethoxide solution. The reaction mixture was further refluxed for 12h and then allowed to cool at 4 °C overnight. Precipitated solids were filtered and washed with cold ethanol to obtain compound **4**{1-7} as white solids.

General procedure for the synthesis of Compound 6{1-7,1-6}. To a solution of compound **4**{1-7}(1 eq.) in anhydrous DMF were added, compound **5**{1-6} (1.1 eq.) and triethylamine (2 eq.). The reaction mixture was heated to dissolve the components and then stirred at room temperature for 10 minutes or until the reaction was complete. The solvent was then removed under vacuum to obtain the residue which was suspended in methanol with sonication. Precipitated solids were filtered and washed with excess methanol to give compound **6**{1-7,1-6} as white solids.

Syntheses of Compounds 9 and 10. These compounds were synthesized in a manner similar to that of the combinatorial library using either pentyl isothiocyante (**7a**) for compound **8a** or hexyl isothiocyanate (**7b**) for compound **8b** and then cyclized and alkylated as described for syntheses

of compounds **6**{1-6,1-7} to give pentyl derivatives **9a** and **9b** and hexyl derivatives **10a** and **10b** respectively.

Syntheses of Compounds 11 and 12. To a solution of compound **6**{7,5} for compound **11** or compound **6**{7,6} for compound **12** (1 eq.) in anhydrous DMF, was added sodium hydride (1.1 eq.) at room temperature. The reaction mixture was stirred for 5 min followed by the addition of iodomethane (1.1 eq.) and stirred for additional 2h. The solvent was then removed under vacuum and the residue was dissolved in ethylacetate, washed with water, dried over sodium sulfate and concentrated to obtain the crude product which was purified using column chromatography to obtain compound **11** or **12**.

Biology

Cell lines and reagents

The CellSensor® NFκB-bla human monocytic THP-1 cell line was purchased from Thermo Fisher Scientific (Waltham, MA). This cell line contains a stably integrated beta-lactamase reporter gene under the control of the Nuclear Factor kappa B (NF-κB) response element (https://tools.thermofisher.com/content/sfs/manuals/CellSensor_NFkBbla_THP1_man.pdf). NF-κB activation results in beta-lactamase production, which shifts the fluorescence emission of the beta-lactamase substrate (LiveBLAzerTM-FRET B/G (CCF4-AM), Thermofisher) to favor coumarin (460 nm emission) over fluorescein (530 nm emission). Murine or human TLR4 HEK Blue™ cells were purchased from Invivogen. These cell lines were stably co-transfected with human or mouse TLR4, MD-2, and CD14 co-receptor genes, and an inducible secreted embryonic alkaline phosphatase (SEAP) reporter gene. QuantiBlue was purchased from Invivogen, MTT (3-[4,5-dimethylthiazol-2-yl]-2,5-dipheyl tetrazolium bromide) was purchased from Acros Organics, and ovalbumin was purchased from Thermo Fisher Scientific. For the HTS

LPS *E. coli 0111:B4* (Sigma Aldrich) was used and LPS-EB Ultrapure (cat# tlrl-3pelps, Invivogen, San Diego CA) was used in the validation and subsequent SAR studies. Wortmannin[33], a non-specific, covalent inhibitor of PI3K, and MPLA was purchased from Invivogen (San Diego, CA).

Measurement of NF-κB activation using CellSensor® NF-κB-bla THP-1

CellSensor® NF-κB-bla THP-1 cells were plated in 96-well plates at 80 µl (5×10^4 cells) per well in RPMI supplemented with 10% dialyzed fetal bovine serum (FBS, Omega Scientific, Inc., Tarzana, CA), 0.1 mM non-essential amino acids, 1 mM sodium pyruvate, 100 U/mL penicillin and100 µg/ml streptomycin (additives from Thermo Fisher Scientific). 10 µl of 10x (50 µM) of compound and 10 µL of 10x (100 ng/ml) LPS-EB in assay media were then added. Cells were incubated for 5h and 20h in 5% CO_2 at 37° C, after which 20 µL of 6xLiveBLAzer™ FRET B/G Substrate (CCF4-AM) mixture (prepared according to the manufacturer's instructions) was added to each well. Plates were incubated at room temperature in the dark for 2h. Fluorescence was measured on a Tecan Infinite M200 plate reader (Männedorf, Switzerland) at an excitation wavelength of 405 nm, and emission wavelengths of 465 nm and 535 nm. Background values (cell free wells at the same fluorescence wavelength) were subtracted from the raw fluorescence intensity values and the emission ratios were calculated as the ratio of background subtracted fluorescence intensities at 465 nm to background subtracted fluorescence intensities at 535 nm. The response ratio was then calculated using the formula: [(emission ratio of a test well)/average emission ratio of wells with vehicle (0.5% DMSO)]. Compounds were ranked using "%act" metrics, which was calculated as [response ratio of the compound/response ratio of LPS]. In each assay, negative control wells were included that were cell-free and cells with vehicle (0.5% DMSO).

Cell viability assays

THP-1 cells were dispensed in 96-well plates (10^5 cells/well) and treated with 5 μM of each compound. After 18h of incubation, a solution of MTT in assay media (0.5 mg/ml) was added to each well and further incubated for 4-6 hours, followed by addition of cell lysis buffer (15% w/v SDS and 0.12% v/v 12N HCl aqueous solution), incubated overnight and then absorbance measured at 570 nm using 650 nm as reference with a plate reader.

In vitro assays using TLR4 reporter cell lines

Murine or human TLR4 HEK Blue™ cells (2.5×10^4 cells per well of a 96 well plate) were incubated with 5 μM of each test compound. The culture supernatants were harvested after a 20-24 h incubation period. SEAP activity in the supernatants was determined using QuantiBlue, and absorbance read at 630 nm per the manufacturer's instructions as previously reported.[7]

Animals

Seven to nine-week-old C57BL/6 (wild-type, WT) mice were purchased from The Jackson Laboratories (Bar Harbor, MA). All animal experiments received prior approval from the UCSD Institutional Animal Care and Use Committee.

In vivo adjuvant activity study

WT mice (n=5 per group) were immunized in the gastronemius muscle with ovalbumin (20 μg/animal) mixed with MPLA (10 μg/animal) and compound **6**{7,5} or **6**{6,6} or **6**{7,6} (100 nmol/animal) on days 0 and 14. On day 21, immunized mice were bled and OVA-specific IgG titers were measured by ELISA as previously described.[47]

Statistical analysis for *in vitro* and *in vivo* studies

Data for *in vitro* and *in vivo* studies are represented as mean ± standard error of the mean (SEM) or mean ± standard deviation (SD). Prism 6 (GraphPad Software, San Diego, CA) statistical

software was used to obtain p-values for comparison between groups ($p<0.05$ was considered significant) for in vivo study. One-way ANOVA followed by Dunn's post hoc test was used to compare multiple groups.

FIGURES

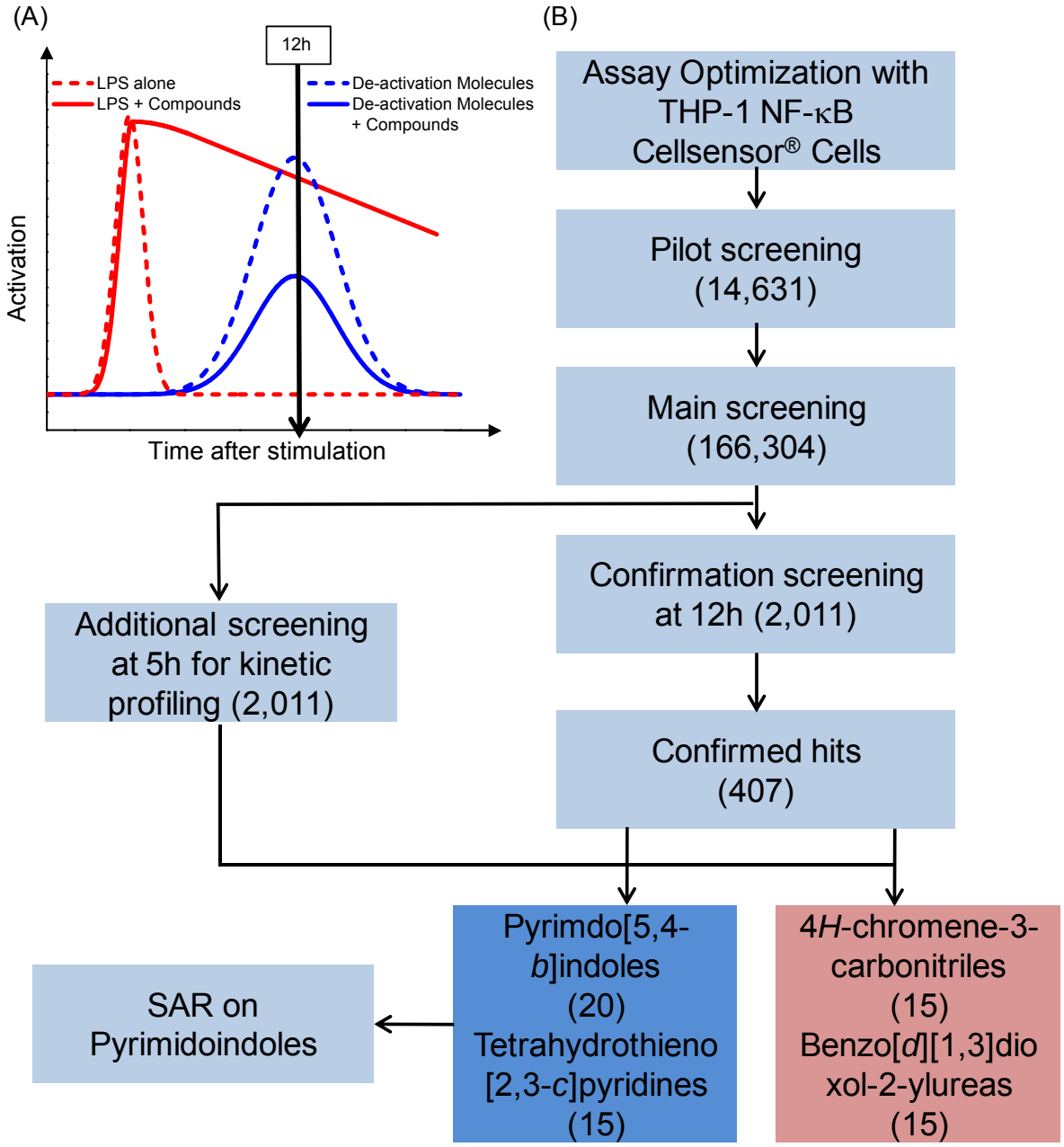

Figure 1. Theoretical kinetics of LPS activation and the HTS workflow strategy. (A) Theoretical kinetic profiles showing activation by LPS (dashed red line) and subsequent deactivation at 12h due to increase in deactivation molecules (dashed blue line). Addition of compounds that prolong

the initial activation (solid red line) and also suppress the formation of deactivation molecules (solid blue line) were identified through HTS. (B) The cell based assay using THP-1 CellSensor® NF-κB reporter cells was optimized for identification of compounds that prolonged NF-κB activation when stimulated with LPS for 12h. The assay was tested in a pilot screen of 14,631 compounds to validate the approach. In the main library screen, 166,304 compounds were screened in the presence of LPS for NF-κB activation at 12h. Cluster based statistical analysis yielded 2,011 compounds, which were retested in a confirmation screen at 12h with LPS in duplicate. An additional screen was performed on these 2,011 compounds for measuring NF-κB activity at 5h to observe the activity kinetics. 407 compounds that had confirmed activity at 12h were structurally clustered using Tanimoto index at 0.5. Four large families of chemotypes were identified as hits based on their kinetic profile of 5h and 12h that prolonged NF-κB activation with LPS. The pyrimidoindole class of compounds was selected for further SAR studies. The number in parentheses corresponds to number of compounds.

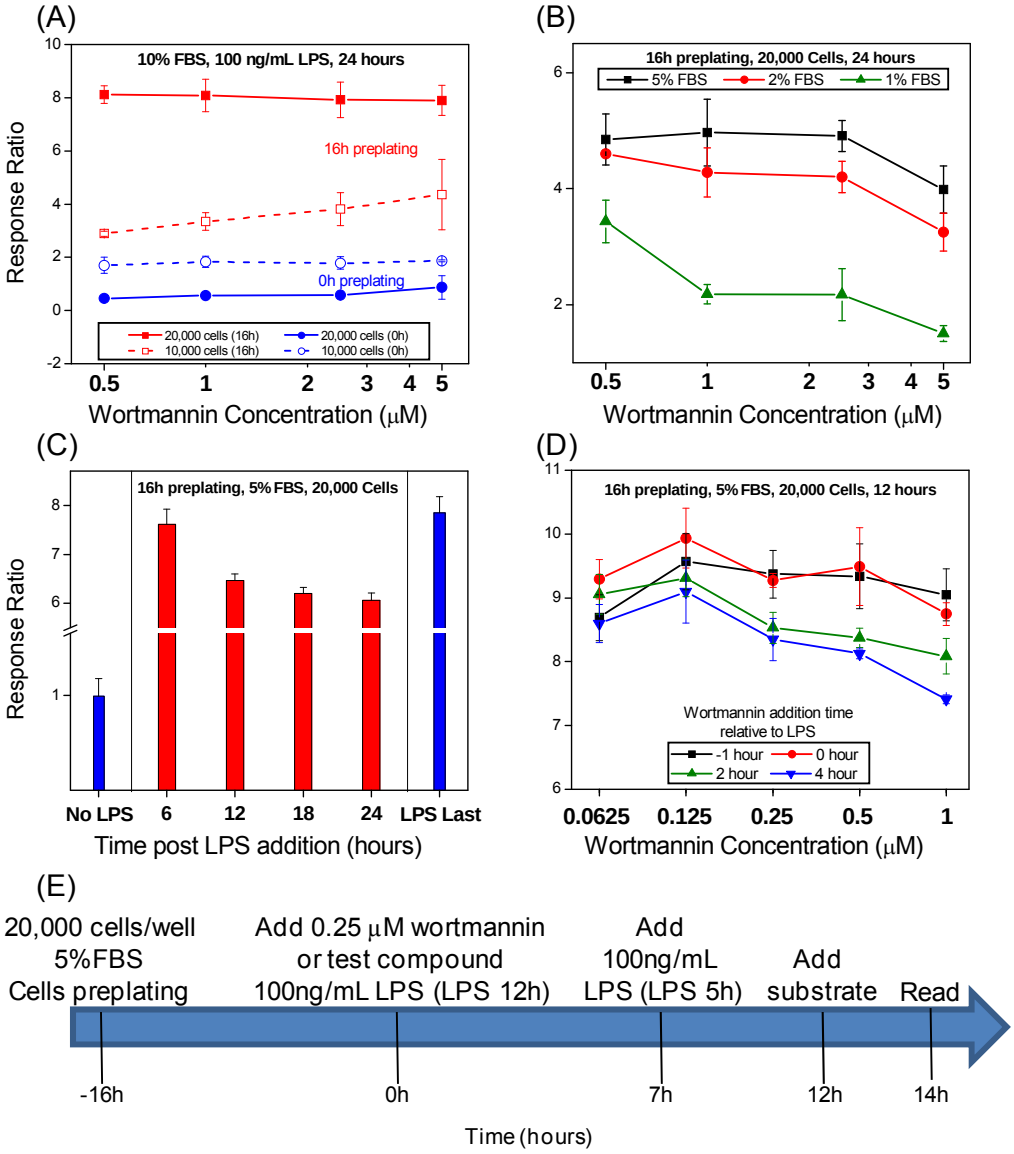

Figure 2. Optimization of assay conditions in THP-1 CellSensor® assay. The assay conditions were optimized for the following parameters: (A) Cell numbers/well and cells preplating time; (B) FBS concentration; (C) incubation time; and (D) concentration of wortmannin and the time of its addition relative to LPS. (E) The schematic shows the optimum assay parameters and the assay protocol used for the HTS. Briefly, the cells were preplated at a density of 20,000 cells/well in 5% FBS 16h prior to addition of 100ng/mL LPS alone or LPS with 0.25μM

wortmannin. An additional control (LPS 5h) was added 5h prior to the addition of FRET substrate at 12h and the plates were read at 14h.

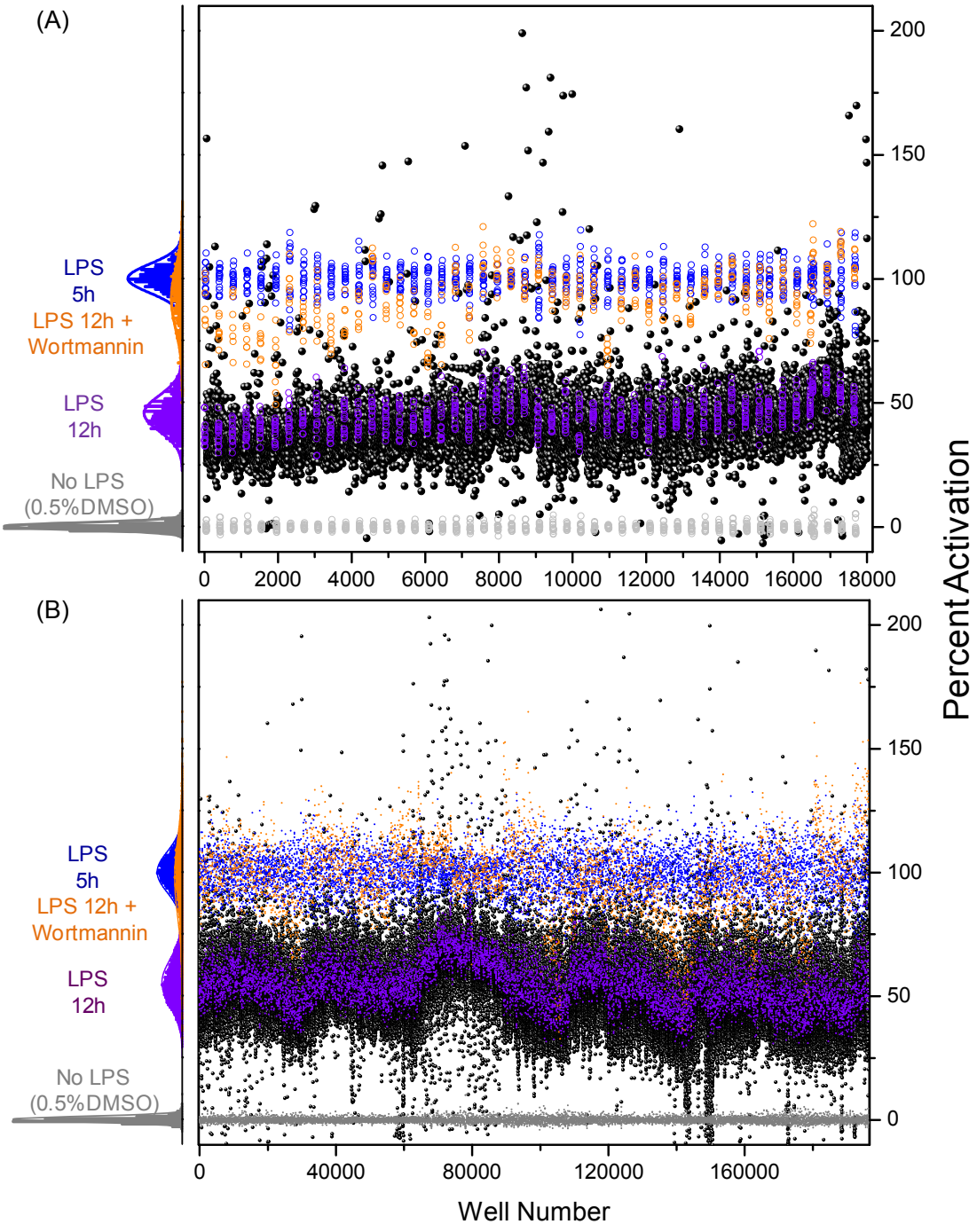

Figure 3. Pilot and HTS main screen. Percent activation values for the controls and test compounds from (A) the pilot screen and (B) the main screen. The histogram plot to the left for each screen shows the intra-assay statistics on the percent activation values for No LPS (0.5%

DMSO, negative control), LPS 12h (100ng/mL LPS control added at time 0h), LPS 12h + wortmannin (positive control), and LPS 5h (100ng/mL LPS control added 5h before the assay read out). The scatter plot to the right shows percent activation values for all the compounds and controls used in each screen. Each black circle represents an individual test compound, while controls are colored as in the histogram plot.

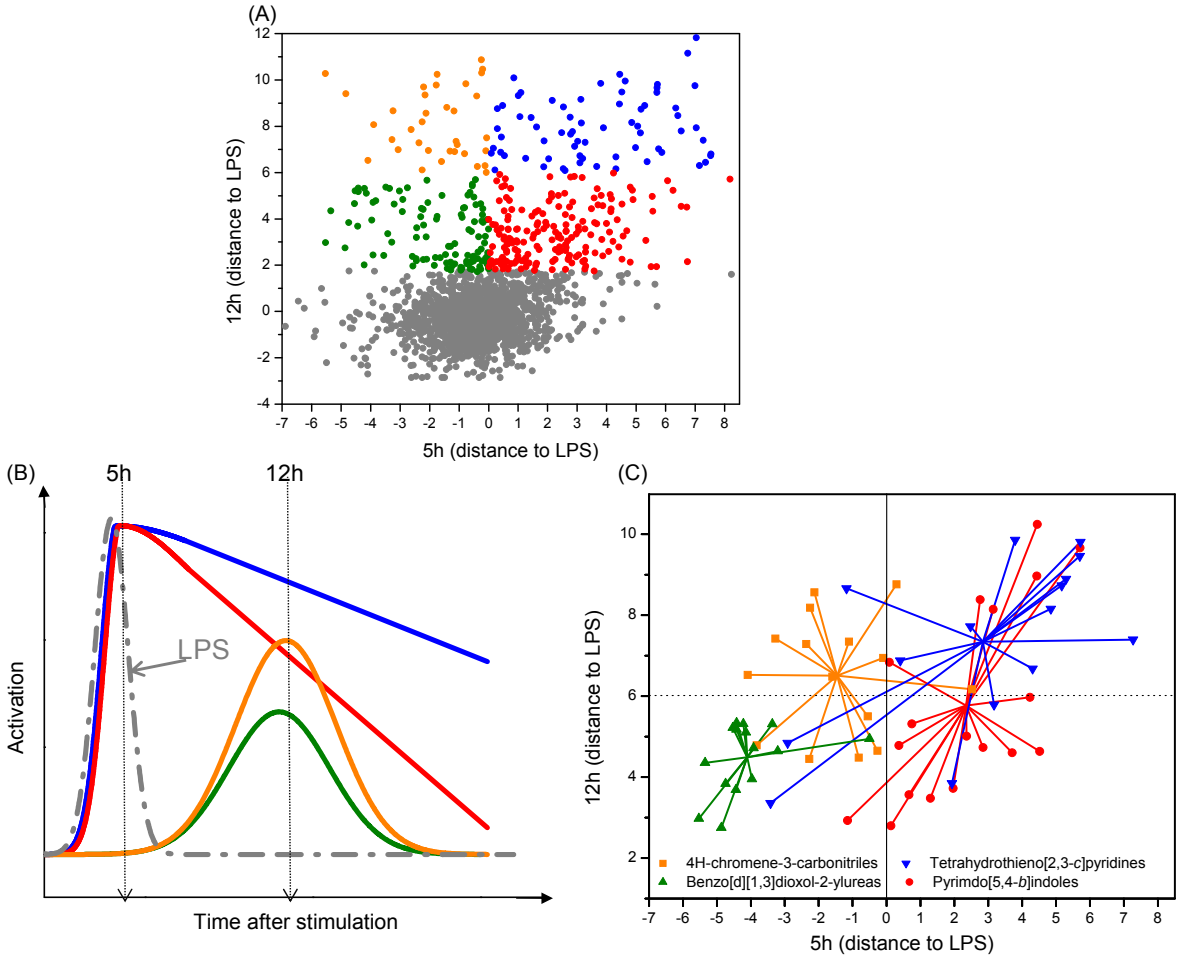

Figure 4. Confirmation and kinetic profile screens. (A) A scatter plot of distance to LPS values for 2,011 compounds selected for confirmation and kinetic profile screens. The abscissa values correspond to kinetic profile experiment while the ordinate values correspond to the confirmation screen experiment. (B) The compounds were divided into four categories based on their theoretical kinetic profiles for NF-κB activation with LPS. These compounds were either early inhibitors (5h distance to LPS<0) or early enhancers (5h distance to LPS>0). Within the early inhibitors, the compounds were grouped as either showing moderate increase or high increase in NF-κB induction compared to LPS at 12h (green and orange symbols and lines, respectively). Similarly, within the enhancer groups, compounds showed moderate or high increase in NF-κB induction compared to LPS at 12h (red and blue symbols and lines, respectively). (C) Cluster

binning of confirmed hits indicates segregation of chemotypes into distinct kinetic profiles. Large clusters were colored based on chemotype, namely pyrimido[5,4-*b*]indoles (red circles), tetrahydrothieno[2,3-*c*]pyridines(blue triangles), benzo[*d*][1,3]dioxol-2-ylureas (green triangles) and 4*H*-chromene-3-carbonitriles (orange squares). The center of the chemotype cluster was calculated as the geometric mean of the coordinates within a cluster. The colors are consistent with the kinetic profiles shown in (B).

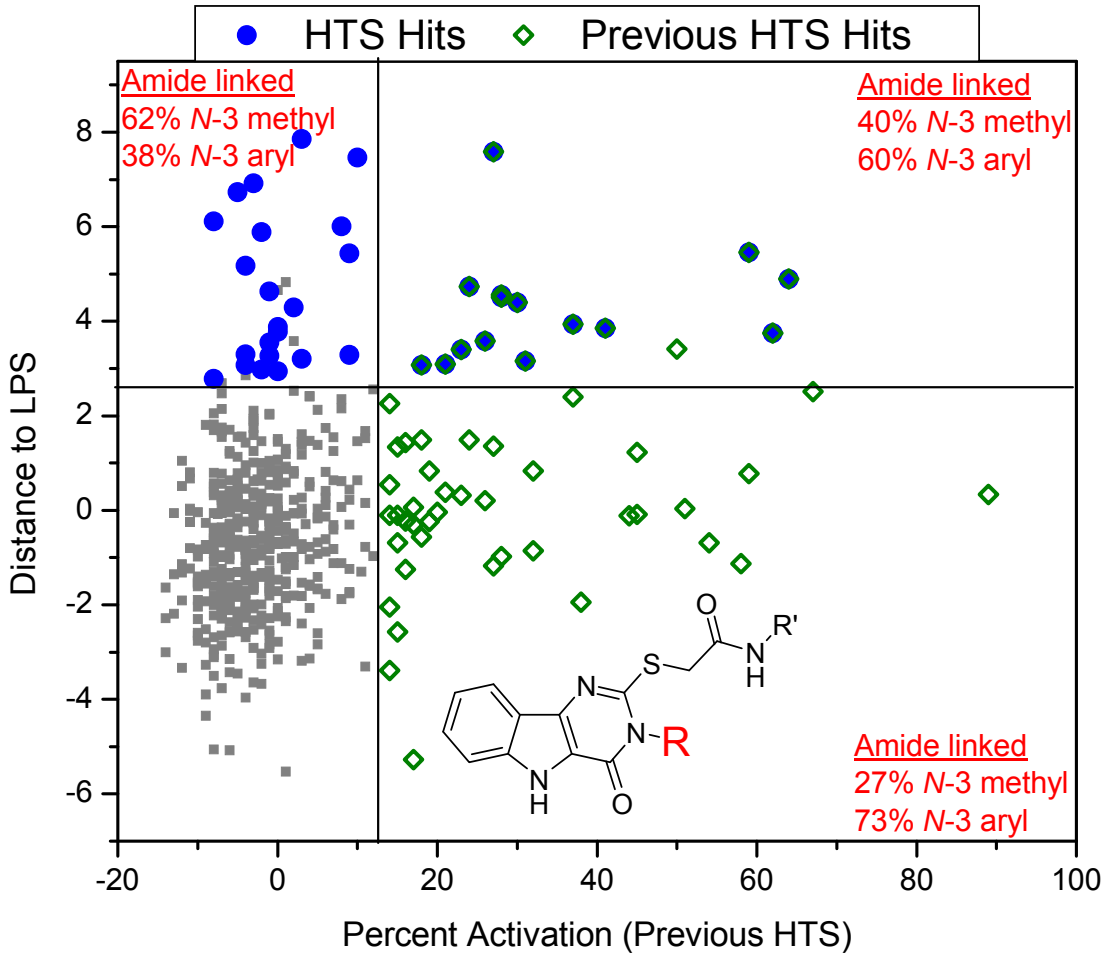

Figure 5. NF-κB activation data for pyrimidoindoles from two different HTS campaigns. A scatter plot of 'distance to LPS' values from the current HTS on Y-axis and 'percent activation' values from the previous HTS on X-axis for all the pyrimidoindoles shows clearly the distinct structural attribute for the C2-S-methylene acetamide linked molecules. The blue circles represent the hits identified in current HTS campaign while the green squares represent the hits identified in the previous HTS. The *N*3-aryl substituted pyrimidoindoles show intrinsic NF-κB activity while *N*3-methyl substituted pyrimidoindoles tend to prolong initial NF-κB activation by LPS without any intrinsic NF-κB activation.

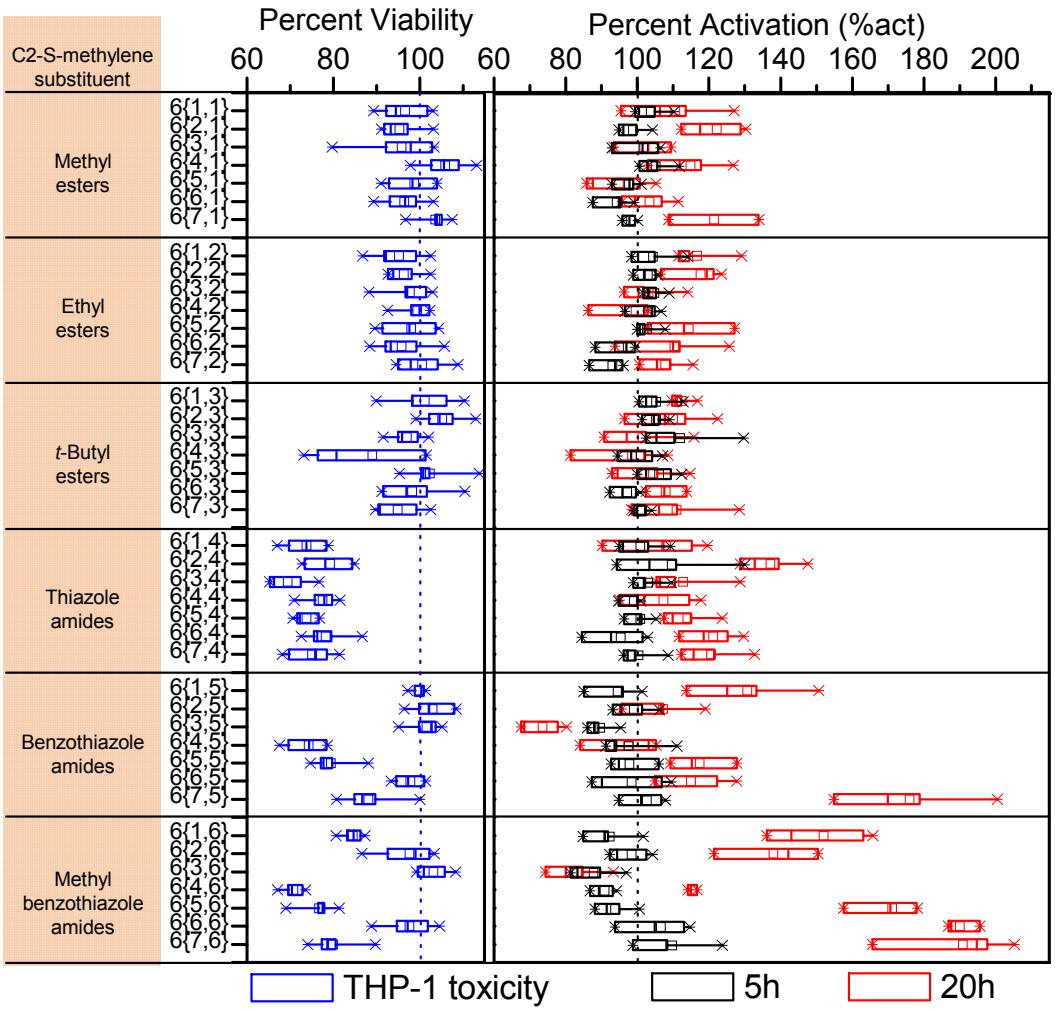

Figure 6. NF-κB induction Assay and MTT toxicity in THP-1 cells. The viability (blue boxes) measured by MTT assay in THP-1 cells relative to DMSO (blue dotted line) and NF-κB percent activation for synthesized pyrimidoindole library compounds in presence of LPS calculated relative to LPS alone (black dotted line) values at both 5h (black boxes) and 12h (red boxes). The values were statistically computed from two and four independent experiments for MTT cell viability and NF-κB activation assays, respectively in THP-1 cells. The C2-S-methylene substituent on the pyrimidoindole for the synthesized compounds is shown in the individual

blocks on the left. Relative viability was calculated as percentage of OD at 630nm compared to DMSO. The OD at 630nm for DMSO was 0.92 ± 0.1 (mean ± SD). Percent activation (%act) was calculated as response ratio relative to LPS. The response ratio for LPS was 8.00 ± 1.2 and 2.58 ± 0.48 at 5h and 20h (mean ± SD), respectively.

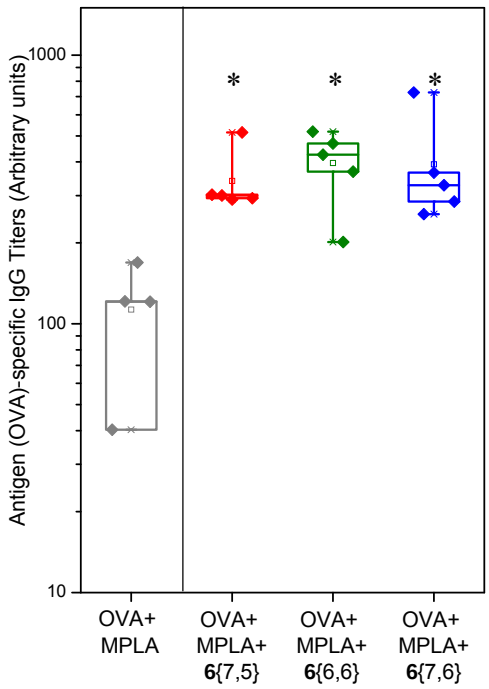

Figure 7. Co-adjuvanticity of potent pyrimidoindole compounds with MPLA. Mice (n=4-5 per group) were immunized on day 0 and day 14 with antigen (ovalbumin, 20µg/animal), MPLA (10µg/animal) and compound **6**{7,5} or **6**{6,6} or **6**{7,6} (100nmol/animal). The immunized mice were bled on day 21 and OVA-specific IgG titers were measured using ELISA. Note, that the potent compounds augmented the production of antigen-specific IgG by approximately 4 fold when co-adjuvanted with MPLA compared to MPLA alone.

*$p<0.05$ compared to OVA+ MPLA group using one-way ANOVA followed by Dunn's post hoc testing.

SCHEMES

Scheme 1. Syntheses of differently *N*3 and C2-substituted pyrimidoindoles.

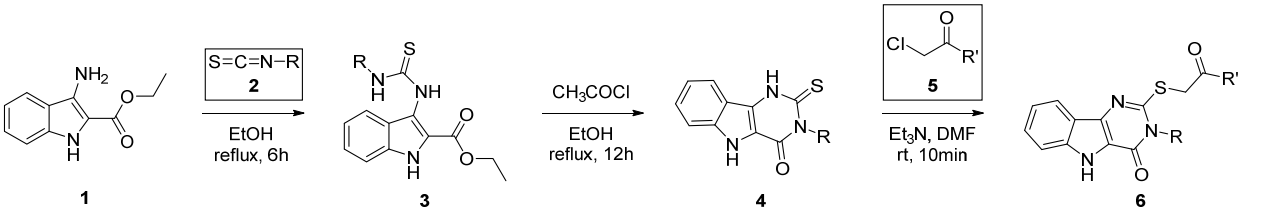

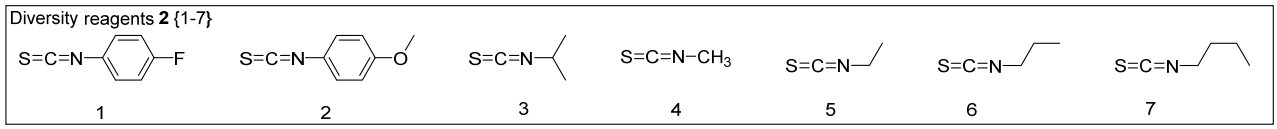

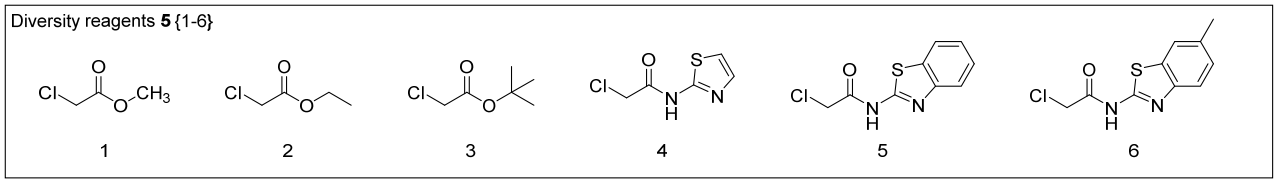

Reagents and conditions: i. **2**, EtOH, 78 °C 6h; ii. CH_3COCl, EtOH, 78 °C, 12h; iii. **5**, Et_3N, DMF, 10min.

Scheme 2. Syntheses of *N*3-pentyl, hexyl, and *N*5-methyl substituted derivatives of select pyrimidoindoles.

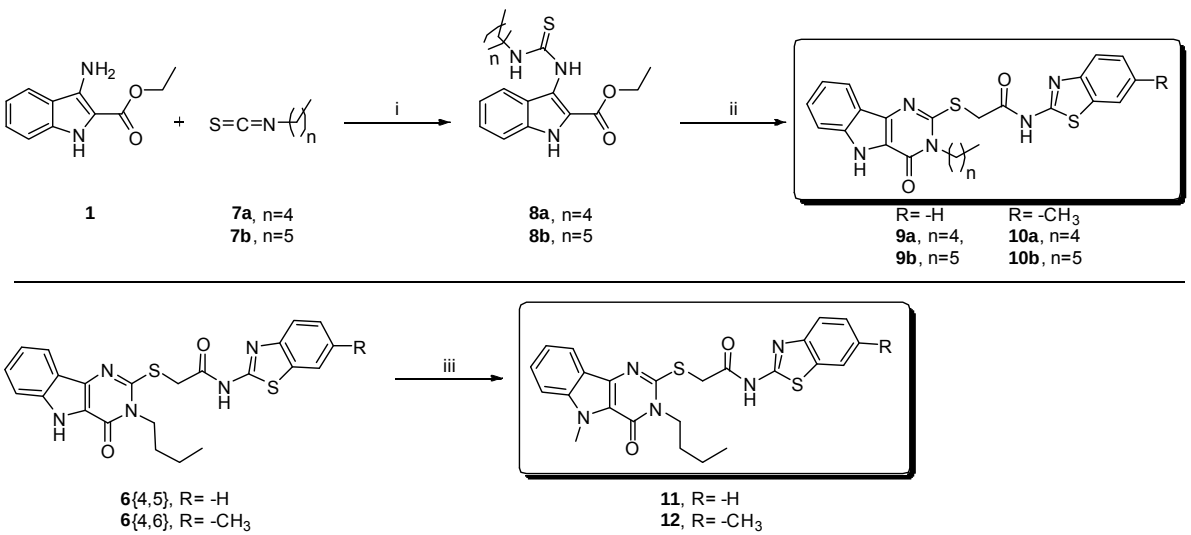

Reagents and conditions: i. EtOH, 78 °C 6h; ii. (a) CH_3COCl, EtOH, 78 °C, 12h; (b) **5**{5} or **5**{6}, Et_3N, DMF, 10min; iii. NaH, CH_3I, DMF, 1h.

ASSOCIATED CONTENT

Supporting Information. The following files are available free of charge.

Supporting Information, Figures S1-S3, Table S1, Chemistry experimental section with compound names, reaction yields, ^{1}H NMR, MS characterization data for all the final compounds as well as ^{13}C NMR and HRMS characterization data for key compounds, ^{1}H NMR and LC-MS spectra for final compounds, ^{13}C NMR and HRMS spectra for key compounds, and detailed synthetic protocol for reagents **5**{4-6} (PDF).

Corresponding Author

*Nikunj M. Shukla, Ph.D.

University of California San Diego

9500 Gilman Drive, #0695

La Jolla, CA 92093-0695

Tel: (858) 534-5424

Fax: (858) 534-8329

E-mail: nishukla@ucsd.edu

Author Contributions

The manuscript was written through contributions by all the authors. All authors approved the final version of the manuscript. KM and MP performed statistical analysis of the HTS data. MC, BN, HC, and NS synthesized compounds. TH, AA, SY, FK, and MCorr performed biological assays. HC and NS performed chemotype clustering analysis. MC, TH, KM, MP, MCorr, DC, HC, and NS wrote the manuscript.

Funding Sources

We acknowledge the NIH Adjuvant Discovery Program for funding (HHSN272200900034C and HHSN272201400051C, Principal Investigator-Dennis A. Carson). The funders had no role in study design, data collection and interpretation, or the decision to submit the work for publication.

Conflict of interest

All authors declare that there is no conflict of interest regarding the publication of this manuscript.

ACKNOWLEDGMENT

We are grateful to Dr. Michael Harvey and his team at the Life Technologies Corporation, Madison, WI for performing the assay optimization, pilot and HTS experiments as well as confirmation and kinetic screens at their facility.

ABBREVIATIONS

APC, antigen presenting cells; DMF, N,N-dimethylformamide; DMSO, dimethyl sulfoxide; ELISA, enzyme-linked immunosorbent assay; FDA, Food and Drug Administration; FRET, Förster resonance energy transfer; HTS, high-throughput screening; Ig, immunoglobulin; IL-10, interleukin-10; IRAK, interleukin-1 receptor-associated kinase; MPLA, monophosphoryl Lipid A; MTT, (3-[4,5-dimethylthiazol-2-yl]-2,5-dipheyl tetrazolium bromide); NF-κB, nuclear factor kappa B; OD, optical density; OVA, ovalbumin; PI3K, phosphatidylinositide-3 kinase; RR, response ratio; SDS, sodium dodecyl sulfate; SEAP, secreted embryonic alkaline phosphatase; TLC, thin layer chromatography; WT, wild type.

TOC GRAPHIC

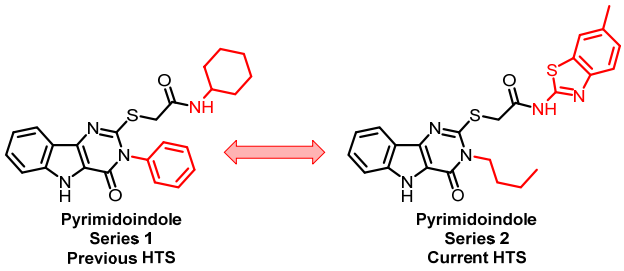

Bio-activity	Series 1	Series 2
Toll-like Receptor 4 Agonist	Yes	No
Intrinsic NF-κB Activity	Yes	No
Sustain NF-κB Activation by LPS	No	Yes

REFERENCES

1. Van Buynder, P. G.; Konrad, S.; Van Buynder, J. L.; Brodkin, E.; Krajden, M.; Ramler, G.; Bigham, M., The comparative effectiveness of adjuvanted and unadjuvanted trivalent inactivated influenza vaccine (TIV) in the elderly. *Vaccine* **2013,** *31* (51), 6122-8.
2. Reed, S. G.; Orr, M. T.; Fox, C. B., Key roles of adjuvants in modern vaccines. *Nature medicine* **2013,** *19* (12), 1597-608.
3. O'Hagan, D. T.; Rappuoli, R.; De Gregorio, E.; Tsai, T.; Del Giudice, G., MF59 adjuvant: the best insurance against influenza strain diversity. *Expert review of vaccines* **2011,** *10* (4), 447-62.
4. Doherty, M.; Schmidt-Ott, R.; Santos, J. I.; Stanberry, L. R.; Hofstetter, A. M.; Rosenthal, S. L.; Cunningham, A. L., Vaccination of special populations: Protecting the vulnerable. *Vaccine* **2016,** *34* (52), 6681-6690.
5. Camilloni, B.; Basileo, M.; Valente, S.; Nunzi, E.; Iorio, A. M., Immunogenicity of intramuscular MF59-adjuvanted and intradermal administered influenza enhanced vaccines in subjects aged over 60: A literature review. *Human vaccines & immunotherapeutics* **2015,** *11* (3), 553-63.
6. Hammer, G. E.; Ma, A., Molecular control of steady-state dendritic cell maturation and immune homeostasis. *Annual review of immunology* **2013,** *31*, 743-91.
7. Chan, M.; Hayashi, T.; Mathewson, R. D.; Nour, A.; Hayashi, Y.; Yao, S.; Tawatao, R. I.; Crain, B.; Tsigelny, I. F.; Kouznetsova, V. L.; Messer, K.; Pu, M.; Corr, M.; Carson, D. A.; Cottam, H. B., Identification of Substituted Pyrimido[5,4-b]indoles as Selective Toll-Like Receptor 4 Ligands. *J. Med. Chem.* **2013,** *56* (11), 4206-4223.
8. Nour, A.; Hayashi, T.; Chan, M.; Yao, S.; Tawatao, R. I.; Crain, B.; Tsigelny, I. F.; Kouznetsova, V. L.; Ahmadiiveli, A.; Messer, K.; Pu, M.; Corr, M.; Carson, D. A.; Cottam, H. B., Discovery of substituted 4-aminoquinazolines as selective Toll-like receptor 4 ligands. *Bioorg. Med. Chem. Lett.* **2014,** *24* (21), 4931-4938.
9. Goff, P. H.; Hayashi, T.; Martinez-Gil, L.; Corr, M.; Crain, B.; Yao, S.; Cottam, H. B.; Chan, M.; Ramos, I.; Eggink, D.; Heshmati, M.; Krammer, F.; Messer, K.; Pu, M.; Fernandez-Sesma, A.; Palese, P.; Carson, D. A., Synthetic Toll-like receptor 4 (TLR4) and TLR7 ligands as influenza virus vaccine adjuvants induce rapid, tained, and broadly protective responses. *J. Virol.* **2015,** *89* (6), 3221-3235.
10. Shukla, N. M.; Salunke, D. B.; Balakrishna, R.; Mutz, C. A.; Malladi, S. S.; David, S. A., Potent adjuvanticity of a pure TLR7-agonistic imidazoquinoline dendrimer. *PLoS One* **2012,** *7* (8), e43612.
11. Salunke, D. B.; Connelly, S. W.; Shukla, N. M.; Hermanson, A. R.; Fox, L. M.; David, S. A., Design and development of stable, water-soluble, human Toll-like receptor 2 specific monoacyl lipopeptides as candidate vaccine adjuvants. *J Med Chem* **2013,** *56* (14), 5885-900.
12. Vasilakos, J. P.; Tomai, M. A., The use of Toll-like receptor 7/8 agonists as vaccine adjuvants. *Expert review of vaccines* **2013,** *12* (7), 809-19.
13. Maisonneuve, C.; Bertholet, S.; Philpott, D. J.; De Gregorio, E., Unleashing the potential of NOD- and Toll-like agonists as vaccine adjuvants. *Proc Natl Acad Sci U S A* **2014,** *111* (34), 12294-9.
14. Basto, A. P.; Leitao, A., Targeting TLR2 for vaccine development. *J Immunol Res* **2014,** *2014*, 619410.

15. Wheeler, C. M.; Skinner, S. R.; Del Rosario-Raymundo, M. R.; Garland, S. M.; Chatterjee, A.; Lazcano-Ponce, E.; Salmeron, J.; McNeil, S.; Stapleton, J. T.; Bouchard, C.; Martens, M. G.; Money, D. M.; Quek, S. C.; Romanowski, B.; Vallejos, C. S.; Ter Harmsel, B.; Prilepskaya, V.; Fong, K. L.; Kitchener, H.; Minkina, G.; Lim, Y. K.; Stoney, T.; Chakhtoura, N.; Cruickshank, M. E.; Savicheva, A.; da Silva, D. P.; Ferguson, M.; Molijn, A. C.; Quint, W. G.; Hardt, K.; Descamps, D.; Suryakiran, P. V.; Karkada, N.; Geeraerts, B.; Dubin, G.; Struyf, F., Efficacy, safety, and immunogenicity of the human papillomavirus 16/18 AS04-adjuvanted vaccine in women older than 25 years: 7-year follow-up of the phase 3, double-blind, randomised controlled VIVIANE study. *The Lancet. Infectious diseases* **2016,** *16* (10), 1154-68.
16. Aoshi, T.; Koyama, S.; Kobiyama, K.; Akira, S.; Ishii, K. J., Innate and adaptive immune responses to viral infection and vaccination. *Current opinion in virology* **2011,** *1* (4), 226-32.
17. Akira, S., Innate immunity and adjuvants. *Philosophical transactions of the Royal Society of London. Series B, Biological sciences* **2011,** *366* (1579), 2748-55.
18. Wang, J.; Hu, Y.; Deng, W. W.; Sun, B., Negative regulation of Toll-like receptor signaling pathway. *Microbes Infect* **2009,** *11* (3), 321-7.
19. Qian, C.; Cao, X., Regulation of Toll-like receptor signaling pathways in innate immune responses. *Ann N Y Acad Sci* **2013,** *1283*, 67-74.
20. Turnis, M. E.; Song, X. T.; Bear, A.; Foster, A. E.; Gottschalk, S.; Brenner, M. K.; Chen, S. Y.; Rooney, C. M., IRAK-M removal counteracts dendritic cell vaccine deficits in migration and longevity. *J Immunol* **2010,** *185* (7), 4223-32.
21. Shembade, N.; Ma, A.; Harhaj, E. W., Inhibition of NF-kappaB signaling by A20 through disruption of ubiquitin enzyme complexes. *Science (New York, N.Y.)* **2010,** *327* (5969), 1135-9.
22. Yuk, J. M.; Shin, D. M.; Lee, H. M.; Kim, J. J.; Kim, S. W.; Jin, H. S.; Yang, C. S.; Park, K. A.; Chanda, D.; Kim, D. K.; Huang, S. M.; Lee, S. K.; Lee, C. H.; Kim, J. M.; Song, C. H.; Lee, S. Y.; Hur, G. M.; Moore, D. D.; Choi, H. S.; Jo, E. K., The orphan nuclear receptor SHP acts as a negative regulator in inflammatory signaling triggered by Toll-like receptors. *Nat Immunol* **2011,** *12* (8), 742-51.
23. Zhou, J.; Wu, R.; High, A. A.; Slaughter, C. A.; Finkelstein, D.; Rehg, J. E.; Redecke, V.; Hacker, H., A20-binding inhibitor of NF-kappaB (ABIN1) controls Toll-like receptor-mediated CCAAT/enhancer-binding protein beta activation and protects from inflammatory disease. *Proc Natl Acad Sci U S A* **2011,** *108* (44), E998-1006.
24. Ho, P. C.; Tsui, Y. C.; Feng, X.; Greaves, D. R.; Wei, L. N., NF-kappaB-mediated degradation of the coactivator RIP140 regulates inflammatory responses and contributes to endotoxin tolerance. *Nat Immunol* **2012,** *13* (4), 379-86.
25. Iwasaki, H.; Takeuchi, O.; Teraguchi, S.; Matsushita, K.; Uehata, T.; Kuniyoshi, K.; Satoh, T.; Saitoh, T.; Matsushita, M.; Standley, D. M.; Akira, S., The IkappaB kinase complex regulates the stability of cytokine-encoding mRNA induced by TLR-IL-1R by controlling degradation of regnase-1. *Nat Immunol* **2011,** *12* (12), 1167-75.
26. An, H.; Zhao, W.; Hou, J.; Zhang, Y.; Xie, Y.; Zheng, Y.; Xu, H.; Qian, C.; Zhou, J.; Yu, Y.; Liu, S.; Feng, G.; Cao, X., SHP-2 phosphatase negatively regulates the TRIF adaptor protein-dependent type I interferon and proinflammatory cytokine production. *Immunity* **2006,** *25* (6), 919-28.
27. An, H.; Hou, J.; Zhou, J.; Zhao, W.; Xu, H.; Zheng, Y.; Yu, Y.; Liu, S.; Cao, X., Phosphatase SHP-1 promotes TLR- and RIG-I-activated production of type I interferon by inhibiting the kinase IRAK1. *Nat Immunol* **2008,** *9* (5), 542-50.

28. O'Neill, L. A.; Sheedy, F. J.; McCoy, C. E., MicroRNAs: the fine-tuners of Toll-like receptor signalling. *Nat Rev Immunol* **2011,** *11* (3), 163-75.
29. Ma, F.; Xu, S.; Liu, X.; Zhang, Q.; Xu, X.; Liu, M.; Hua, M.; Li, N.; Yao, H.; Cao, X., The microRNA miR-29 controls innate and adaptive immune responses to intracellular bacterial infection by targeting interferon-gamma. *Nat Immunol* **2011,** *12* (9), 861-9.
30. Ma, F.; Liu, X.; Li, D.; Wang, P.; Li, N.; Lu, L.; Cao, X., MicroRNA-466l upregulates IL-10 expression in TLR-triggered macrophages by antagonizing RNA-binding protein tristetraprolin-mediated IL-10 mRNA degradation. *J Immunol* **2010,** *184* (11), 6053-9.
31. Liu, X.; Zhan, Z.; Xu, L.; Ma, F.; Li, D.; Guo, Z.; Li, N.; Cao, X., MicroRNA-148/152 impair innate response and antigen presentation of TLR-triggered dendritic cells by targeting CaMKIIalpha. *J Immunol* **2010,** *185* (12), 7244-51.
32. El Gazzar, M.; Church, A.; Liu, T.; McCall, C. E., MicroRNA-146a regulates both transcription silencing and translation disruption of TNF-alpha during TLR4-induced gene reprogramming. *J Leukoc Biol* **2011,** *90* (3), 509-19.
33. Arcaro, A.; Wymann, M. P., Wortmannin is a potent phosphatidylinositol 3-kinase inhibitor: the role of phosphatidylinositol 3,4,5-trisphosphate in neutrophil responses. *Biochem J* **1993,** *296 (Pt 2)*, 297-301.
34. Naiki, Y.; Michelsen, K. S.; Zhang, W.; Chen, S.; Doherty, T. M.; Arditi, M., Transforming growth factor-beta differentially inhibits MyD88-dependent, but not TRAM- and TRIF-dependent, lipopolysaccharide-induced TLR4 signaling. *J Biol Chem* **2005,** *280* (7), 5491-5.
35. Kondo, T.; Kawai, T.; Akira, S., Dissecting negative regulation of Toll-like receptor signaling. *Trends Immunol* **2012,** *33* (9), 449-58.
36. Sakamoto, H.; Egashira, S.; Saito, N.; Kirisako, T.; Miller, S.; Sasaki, Y.; Matsumoto, T.; Shimonishi, M.; Komatsu, T.; Terai, T.; Ueno, T.; Hanaoka, K.; Kojima, H.; Okabe, T.; Wakatsuki, S.; Iwai, K.; Nagano, T., Gliotoxin suppresses NF-kappaB activation by selectively inhibiting linear ubiquitin chain assembly complex (LUBAC). *ACS Chem Biol* **2015,** *10* (3), 675-81.
37. Peng, Y. M.; Zheng, J. B.; Zhou, Y. B.; Li, J., Characterization of a novel curcumin analog P1 as potent inhibitor of the NF-kappaB signaling pathway with distinct mechanisms. *Acta Pharmacol Sin* **2013,** *34* (7), 939-50.
38. Ma, Y. M.; Peng, Y. M.; Zhu, Q. H.; Gao, A. H.; Chao, B.; He, Q. J.; Li, J.; Hu, Y. H.; Zhou, Y. B., Novel CHOP activator LGH00168 induces necroptosis in A549 human lung cancer cells via ROS-mediated ER stress and NF-kappaB inhibition. *Acta Pharmacol Sin* **2016,** *37* (10), 1381-1390.
39. Li, G.; Diogo, D.; Wu, D.; Spoonamore, J.; Dancik, V.; Franke, L.; Kurreeman, F.; Rossin, E. J.; Duclos, G.; Hartland, C.; Zhou, X.; Li, K.; Liu, J.; De Jager, P. L.; Siminovitch, K. A.; Zhernakova, A.; Raychaudhuri, S.; Bowes, J.; Eyre, S.; Padyukov, L.; Gregersen, P. K.; Worthington, J.; Gupta, N.; Clemons, P. A.; Stahl, E.; Tolliday, N.; Plenge, R. M., Human genetics in rheumatoid arthritis guides a high-throughput drug screen of the CD40 signaling pathway. *PLoS Genet* **2013,** *9* (5), e1003487.
40. Jiang, X.; Lv, B.; Li, P.; Ma, X.; Wang, T.; Zhou, Q.; Wang, X.; Gao, X., Bioactivity-integrated UPLC/Q-TOF-MS of Danhong injection to identify NF-kappaB inhibitors and anti-inflammatory targets based on endothelial cell culture and network pharmacology. *J Ethnopharmacol* **2015,** *174*, 270-6.

41. Beck, A.; Vinik, Y.; Shatz-Azoulay, H.; Isaac, R.; Streim, S.; Jona, G.; Boura-Halfon, S.; Zick, Y., Otubain 2 is a novel promoter of beta cell survival as revealed by siRNA high-throughput screens of human pancreatic islets. *Diabetologia* **2013,** *56* (6), 1317-26.
42. Pu, M.; Hayashi, T.; Cottam, H.; Mulvaney, J.; Arkin, M.; Corr, M.; Carson, D.; Messer, K., Analysis of high-throughput screening assays using cluster enrichment. *Stat Med* **2012,** *31* (30), 4175-89.
43. Fukao, T.; Tanabe, M.; Terauchi, Y.; Ota, T.; Matsuda, S.; Asano, T.; Kadowaki, T.; Takeuchi, T.; Koyasu, S., PI3K-mediated negative feedback regulation of IL-12 production in DCs. *Nat Immunol* **2002,** *3* (9), 875-881.
44. Guha, M.; Mackman, N., The Phosphatidylinositol 3-Kinase-Akt Pathway Limits Lipopolysaccharide Activation of Signaling Pathways and Expression of Inflammatory Mediators in Human Monocytic Cells. *Journal of Biological Chemistry* **2002,** *277* (35), 32124-32132.
45. Hazeki, K.; Kinoshita, S.; Matsumura, T.; Nigorikawa, K.; Kubo, H.; Hazeki, O., Opposite effects of wortmannin and 2-(4-morpholinyl)-8-phenyl-1(4H)-benzopyran-4-one hydrochloride on toll-like receptor-mediated nitric oxide production: negative regulation of nuclear factor-{kappa}B by phosphoinositide 3-kinase. *Mol Pharmacol* **2006,** *69* (5), 1717-24.
46. Grün, B.; Leisch, F., FlexMix Version 2: Finite Mixtures with Concomitant Variables and Varying and Constant Parameters. *Journal of Statistical Software; Vol 1, Issue 4 (2008)* **2008**.
47. Chan, M.; Hayashi, T.; Kuy, C. S.; Gray, C. S.; Wu, C. C. N.; Corr, M.; Wrasidlo, W.; Cottam, H. B.; Carson, D. A., Synthesis and Immunological Characterization of Toll-Like Receptor 7 Agonistic Conjugates. *Bioconjugate Chem.* **2009,** *20* (6), 1194-1200.